

LETTER TO THE EDITOR

Ejected-energy differential cross sections for the electron-impact detachment of H^-

M S Pindzola and F Robicheaux

Department of Physics, Auburn University, Auburn, AL 36849, USA

Received 22 February 2000

Abstract. Electron-impact detachment cross sections for H^- are calculated using time-dependent close-coupling theory. The three-electron wavefunction is expanded in terms of a product of a frozen core $1s$ hydrogenic wavefunction and a correlated two-electron wavefunction which fully describes the ejected and scattered electrons at all times following the collision. Ejected-energy differential and total integrated cross sections are calculated at 10 eV and 20 eV incident electron energy. Equal energy anomalies in the differential cross section are avoided by direct projection of the time-dependent wavefunction onto lattice continuum eigenstates. The total cross sections are in excellent agreement with previous ion storage ring experiments, while the differential cross section results confirm Monte Carlo perturbation theory in predicting a zero energy signature which should be common to all negative ions.

Renewed theoretical interest in electron-impact detachment of negative ions has been sparked by recent high precision experimental measurements using ion storage rings [1–4]. The final quantum state after detachment consists of two free electrons moving in the field of a neutral third body. This is qualitatively different from the final quantum state after ionization of an atom or positive ion, in which two free electrons move in the long range Coulomb field of a charged third body. However, common to both the detachment and ionization processes is the difficult task of representing the double-electron continuum. Classical [1] and semiclassical [5–7] approaches have been invoked to predict electron-impact detachment cross sections for negative ions. Fully quantal approaches have used non-perturbative R -matrix theory [8], standard first-order perturbation theory [9], and non-standard first-order perturbation theory based on Monte Carlo integration of a scattering amplitude in a mixed coordinate system [10, 11].

In this letter we apply time-dependent close-coupling (TDCC) theory to the electron-impact detachment of H^- . This fully quantal non-perturbative method has been used previously to calculate electron-impact ionization cross sections for a number of atoms [12, 13] and positive ions [14–17]. To support experiment and to verify the predictions of Monte Carlo perturbation theory (MCPT), we calculate ejected-energy differential and total integrated cross sections for the detachment of H^- at 10 eV and 20 eV incident energy. In the past, the calculation of ejected-energy differential ionization cross sections has presented problems for various non-perturbative quantal treatments, such as the R -matrix pseudo-state [18], converged close-coupling [19, 20], and hyperspherical close-coupling [21] methods. The problems appear to be connected with extraction of differential cross sections by boundary matching of the wavefunction [21, 22]. Non-perturbative methods that avoid asymptotic forms, such as the complex exterior scaling [23] and the time-dependent close-coupling methods, are also found to avoid these equal energy anomalies in the differential cross section.

The time-dependent close-coupling calculations begin with a frozen core 1s hydrogenic wavefunction. A set of bound $\bar{n}l$ and continuum $\bar{k}l$ radial orbitals are then obtained by diagonalization of the single particle Hamiltonian given by:

$$h(r) = -\frac{1}{2} \frac{\partial^2}{\partial r^2} + \frac{l(l+1)}{r^2} - \frac{1}{r} + V_D(r) + V_X(r), \quad (1)$$

where the direct, $V_D(r)$, and local exchange, $V_X(r)$, potentials are calculated using the frozen core 1s orbital (atomic units are used throughout unless otherwise specified). Diagonalization is on a radial grid of 300 points with a uniform mesh spacing of $\Delta r = 0.20$. A parameter in the local exchange potential is adjusted so that the $\bar{1}s$ orbital has a binding energy of -0.75 eV, in agreement with experiment. The $\bar{1}s$ orbital is quite different from the 1s orbital, with a mean radius of $\langle r \rangle = 3.19$, in contrast to the hydrogenic value of $\langle r \rangle = 1.50$.

The total three-electron wavefunction ($e^- + H^-$ system) for a given ${}^2\mathcal{L}$ symmetry is expanded as a coupled product of a frozen core 1s wavefunction and a correlated two-electron wavefunction. Reduction of the time-dependent Schrodinger equation [12, 13] yields two uncoupled sets of close-coupled partial differential equations for each ${}^2\mathcal{L}$ symmetry given by:

$$i \frac{\partial P_{l_1 l_2}^{LS}(r_1, r_2, t)}{\partial t} = T_{l_1 l_2}(r_1, r_2) P_{l_1 l_2}^{LS}(r_1, r_2, t) + \sum_{l'_1 l'_2} U_{l_1 l_2, l'_1 l'_2}^L(r_1, r_2) P_{l'_1 l'_2}^{LS}(r_1, r_2, t), \quad (2)$$

where $P_{l_1 l_2}^{LS}$ is a two-electron radial wavefunction, $L = \mathcal{L}$, $S = 0$ or $S = 1$, and (l_1, l_2) are the angular momenta for the ejected and scattered electrons. The operator $T_{l_1 l_2}$ contains kinetic energy, centrifugal barrier, nuclear, frozen core direct and frozen core exchange terms. The operator $U_{l_1 l_2, l'_1 l'_2}^L$ couples the various (l_1, l_2) scattering channels.

At a time $t = 0$ before the collision, the two-electron radial wavefunctions are taken to be $S = 0$ symmetric or $S = 1$ antisymmetric products of the $\bar{1}s$ radial orbital and an incoming radial wavepacket for the $l = \mathcal{L}$ incident electron. Finite differencing methods are used to represent the close-coupled partial differential equations (equation (2)) on a 300×300 point numerical lattice with a uniform mesh spacing of $\Delta r_1 = \Delta r_2 = 0.20$. The lattice wavefunction is partitioned over the many processors of a distributed memory parallel computer. Each radial wavefunction is propagated in time using an explicit second-order differencing scheme. At a time $t = T$ following the collision the two-electron radial wavefunctions may be projected onto the lone $\bar{1}s$ bound radial orbital or onto the many $\bar{k}l$ continuum radial orbitals. By unitarity, both projection schemes will yield the same total integrated detachment cross section.

For ejected-energy differential detachment cross sections the two-electron radial wavefunctions are projected onto the $\bar{k}l$ continuum radial orbitals to yield momentum space probabilities [13]. In the (k_1, k_2) plane the momentum space probabilities are peaked along a ridge of total energy $E = k_1^2/2 + k_2^2/2 = E_0 - I_p$, where E_0 is the incident energy and I_p is the ionization potential. The diagonalization of $h(r)$ of equation (1) determines the density of states. To increase the density of states at low energies we extended the radial grid to 1500 points, while maintaining the same uniform mesh spacing of $\Delta r = 0.20$. Dividing the (k_1, k_2) plane into angular segments, $\Delta\theta$, defined by the hyperspherical angle $\tan(\theta) = \frac{k_2}{k_1}$, the differential cross section is given by:

$$\frac{\Delta\sigma}{\Delta\theta} = \frac{\pi}{8E_0\Delta\theta} \sum_{LS} (2L+1)(2S+1) \times \sum_{l_1, l_2} \sum_{k_1, k_2} \left| \int_0^\infty dr_1 \int_0^\infty dr_2 P_{k_1 \bar{l}_1}(r_1) P_{k_2 \bar{l}_2}(r_2) P_{l_1 l_2}^{LS}(r_1, r_2, t) \right|^2, \quad (3)$$

Table 1. Total integrated partial-wave cross sections (10^{-18} cm²) for the detachment of H⁻ (\mathcal{L} is the total angular momentum and E_0 is the incident energy).

\mathcal{L}	TDCC	MCPT	TDCC	MCPT
	$E_0 = 10$ eV	$E_0 = 10$ eV	$E_0 = 20$ eV	$E_0 = 20$ eV
0	51	242	35	122
1	171	189	85	83
2	214	208	117	106
3	248	253	140	137
4	251	269	149	169
5	241	245	153	159
6	224	238	151	150
7	206	196	146	145
8	189	167	140	140
0–8	1795	2007	1116	1211
0–50	3060	3272	2927	3022

where the sum over linear momenta is restricted to be within:

$$\theta - \frac{\Delta\theta}{2} < \tan^{-1} \left(\frac{k_2}{k_1} \right) < \theta + \frac{\Delta\theta}{2}. \quad (4)$$

The differential cross section in ejected energy ($\epsilon = \frac{k_2^2}{2}$) is given by:

$$\frac{d\sigma}{d\epsilon} = \frac{1}{k_1 k_2} \frac{d\sigma}{d\theta}, \quad (5)$$

and the total integrated cross section is given by:

$$\sigma = \int_0^E \frac{d\sigma}{d\epsilon} d\epsilon. \quad (6)$$

Total integrated partial-wave cross sections for the electron-impact detachment of H⁻ are presented in table 1 at 10 eV and 20 eV incident electron energy. The time-dependent close-coupling results are found to be in very good agreement with previous Monte Carlo perturbation theory [10, 11] results for $1 \leq \mathcal{L} \leq 8$. For $\mathcal{L} = 0$ the time-dependent close-coupling results are substantially below the unitary limit of $\sigma_{\max} = \frac{\pi}{2E_0}$ ($\sigma_{\max} = 120$ Mb for $E_0 = 10$ eV and half that for $E_0 = 20$ eV), while the Monte Carlo perturbation theory results are substantially above. Obviously the $\mathcal{L} = 0$ MCPT results are incorrect[†]. We note that the differences in the $\mathcal{L} = 0$ –8 totals for the TDCC and MCPT calculations are in large part due to the $\mathcal{L} = 0$ discrepancy. To compare with previous ion storage ring experiments for the total integrated detachment cross section, the low \mathcal{L} partial-wave TDCC and MCPT results are augmented with first-order distorted-wave theory [24] calculations for the high \mathcal{L} partial-wave cross sections. The first-order scattering amplitude is calculated keeping only the direct dipole terms. The incident and scattered electrons are generated in a V^N potential, while the $\bar{1}$ s target and ejected electrons are generated in the V^{N-1} potential found in equation (1). The $\mathcal{L} = 0$ –50 hybrid results for both the TDCC and MCPT methods fall well within the error bars of the ion storage ring experimental measurements [1, 2] of $\sigma_{\text{expt}} = 3000$ Mb \pm 900 Mb at $E_0 = 10$ eV and $\sigma_{\text{expt}} = 2950$ Mb \pm 900 Mb at $E_0 = 20$ eV.

[†] The MCPT calculations fail at $\mathcal{L} = 0$ because the incident electron penetrates to smaller distances before detaching the bound electron. Thus, the electrons in the final state are affected by the short range $e^- + \text{H}$ potential which is neglected in the final state of the MCPT approximation. Numerical tests have shown that the sensitivity to the distorted-wave potential is an order of magnitude smaller for $\mathcal{L} = 1$ than for $\mathcal{L} = 0$.

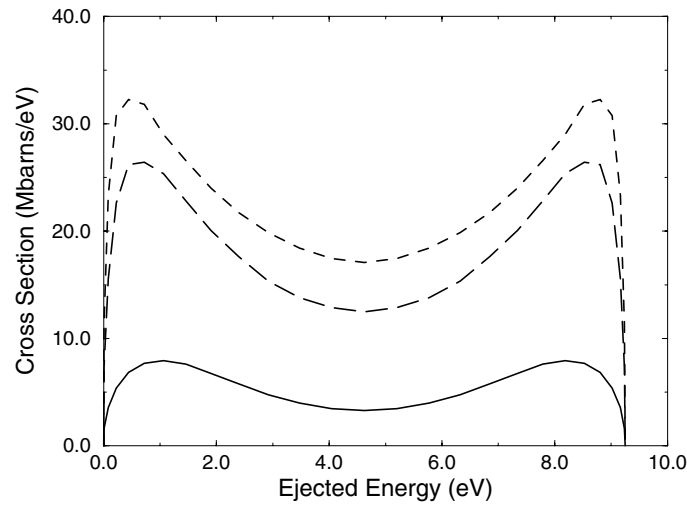


Figure 1. Partial ejected-energy differential cross section for the electron-impact ionization of H^- at an incident energy of 10 eV. Solid curve, S wave; long-dashed curve, P wave; short-dashed curve, D wave (1.0 Mbarn = 1.0×10^{-18} cm²).

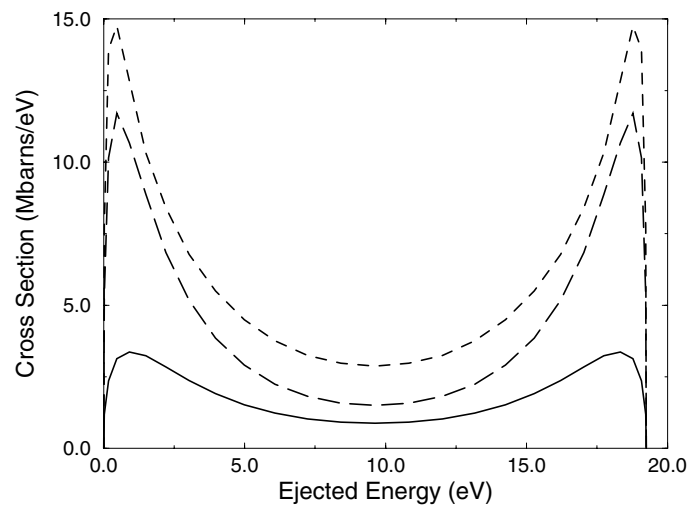


Figure 2. Partial ejected-energy differential cross section for the electron-impact ionization of H^- at an incident energy of 20 eV. Solid curve, S wave; long-dashed curve, P wave; short-dashed curve, D wave (1.0 Mbarn = 1.0×10^{-18} cm²).

Ejected-energy differential partial-wave cross sections for the electron-impact detachment of H^- are presented in figures 1 and 2 at 10 eV and 20 eV incident electron energy. The threshold law for differential detachment of H^- is found to be quite different from the threshold law for differential ionization of an atom or positive ion. For the latter, the zero energy cross section is large, while for the former the cross section is zero. At very low ejected energies the loosely bound electron of H^- is unable to scatter and detach in the neutral field of H, while a bound

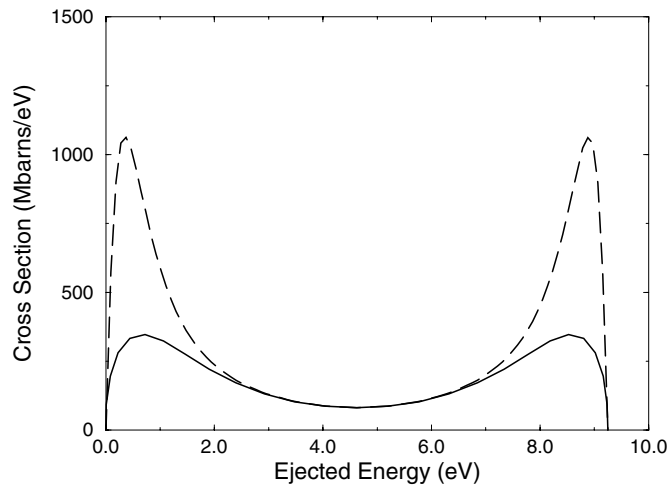


Figure 3. Total ejected-energy differential cross section for the electron-impact ionization of H^- at an incident energy of 10 eV. Solid curve, TDCC for $\mathcal{L} \leq 8$; dashed curve, TDCC for $\mathcal{L} \leq 8$ plus distorted-wave theory for $9 \leq \mathcal{L} \leq 50$ (1.0 Mbarn = 1.0×10^{-18} cm²).

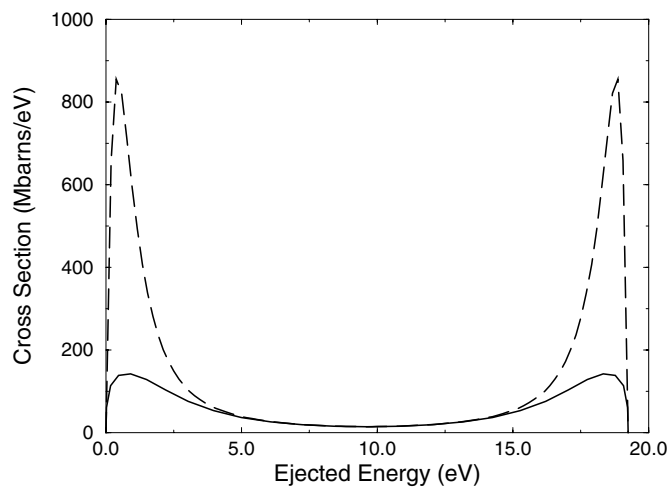


Figure 4. Total ejected-energy differential cross section for the electron-impact ionization of H^- at an incident energy of 20 eV. Solid curve, TDCC for $\mathcal{L} \leq 8$; dashed curve, TDCC for $\mathcal{L} \leq 8$ plus distorted-wave theory for $9 \leq \mathcal{L} \leq 50$ (1.0 Mbarn = 1.0×10^{-18} cm²).

electron of an atom (or positive ion) is able to ionize due to the long range Coulomb field of the residual ion. To stimulate further studies of the electron-impact detachment process in H^- , we present ejected-energy differential cross sections summed over partial waves in figures 3 and 4. The solid curves represent TDCC results for $\mathcal{L} = 0-8$, while the dashed curves include the addition of first-order distorted-wave results for $\mathcal{L} = 9-50$. As pointed out by Robicieux [10, 11], the zero-energy signature in the ejected-energy differential cross section should be common to all negative ions.

In summary, we have calculated the ejected-energy differential and total integrated cross sections for the electron-impact detachment of H^- using time-dependent close-coupling theory. The total wavefunction for the $e^- + H^-$ system is expanded as a coupled product of the $1s$ wavefunction for H and a correlated two-electron wavefunction for the ejected and scattered electrons. Projection of the time-evolved wavefunction onto lattice continuum eigenstates yields ejected-energy differential cross sections free of equal energy anomalies. The time-dependent close-coupling results for the total and differential cross sections are in very good agreement with previous Monte Carlo perturbation theory results. Since the TDCC and MCPT methods treat the detachment process using quite different numerical approaches, their fine agreement is a solid confirmation of both sets of results. When augmented with first-order distorted-wave results for high partial waves, the TDCC and MCPT results are in excellent agreement with ion storage ring experiments for the total integrated detachment cross section. We hope the predicted differential detachment cross sections for H^- can also be checked by future experiments.

This work was supported in part by the US Department of Energy and the US National Science Foundation. Computational work was carried out at the National Energy Research Supercomputer Center in Berkeley, CA.

References

- [1] Andersen L H, Mathur D, Schmidt H T and Vejby-Christensen L 1996 *Phys. Rev. Lett.* **74** 892–5
- [2] Vejby-Christensen L, Kella D, Mathur D, Pedersen H B, Schmidt H T and Andersen L H 1996 *Phys. Rev. A* **53** 2371–8
- [3] Tanbe T *et al* 1996 *Phys. Rev. A* **54** 4069–72
- [4] Andersen L H, Jensen M J, Pedersen H B, Vejby-Christensen L and Djuric N 1998 *Phys. Rev. A* **58** 2819–23
- [5] Ostrovsky V N and Taulbjerg K 1996 *J. Phys. B: At. Mol. Opt. Phys.* **29** 2573–87
- [6] Kazansky A K and Taulbjerg K 1996 *J. Phys. B: At. Mol. Opt. Phys.* **29** 4465–75
- [7] Lin J T, Jiang T F and Lin C D 1996 *J. Phys. B: At. Mol. Opt. Phys.* **29** 6175–84
- [8] Robicheaux F, Wood R P and Greene C H 1994 *Phys. Rev. A* **49** 1866–74
- [9] Pindzola M S 1996 *Phys. Rev. A* **54** 3671–73
- [10] Robicheaux F 1999 *Phys. Rev. Lett.* **82** 707–10
- [11] Robicheaux F 1999 *Phys. Rev. A* **60** 1206–15
- [12] Pindzola M S and Robicheaux F 1996 *Phys. Rev. A* **54** 2142–45
- [13] Pindzola M S and Robicheaux F 2000 *Phys. Rev. A* **61** 052707
- [14] Pindzola M S, Robicheaux F, Badnell N R and Gorczyca T W 1997 *Phys. Rev. A* **56** 1994–9
- [15] Badnell N R, Pindzola M S, Bray I and Griffin D C 1998 *J. Phys. B: At. Mol. Opt. Phys.* **31** 911–24
- [16] Mitnik D M, Pindzola M S, Griffin D C and Badnell N R 1999 *J. Phys. B: At. Mol. Opt. Phys.* **32** L479–85
- [17] Pindzola M S, Mitnik D M, Colgan J and Griffin D C 2000 *Phys. Rev. A* **61** 052712
- [18] Bartschat K and Bray I 1996 *Phys. Rev. A* **54** R1002–5
- [19] Bray I 1997 *Phys. Rev. Lett.* **78** 4721–4
- [20] Bray I 1999 *Phys. Rev. A* **60** 5118–21
- [21] Miyashita N, Kato D and Watanabe S 1999 *Phys. Rev. A* **59** 4385–89
- [22] Rescigno T N, McCurdy C W, Isaacs W A and Baertschy M 1999 *Phys. Rev. A* **60** 3740–9
- [23] McCurdy C W, Rescigno T N and Byrum D 1997 *Phys. Rev. A* **56** 1958–69
- [24] Younger S M 1985 *Electron-Impact Ionization* ed T D Mark and G H Dunn (Berlin: Springer) pp 1–23